NASA TECHNICAL MEMORANDUM

PERFORMANCE AND STALL LIMITS OF A YTF30-P-1 TURBOFAN ENGINE WITH UNIFORM INLET FLOW

by Willis M. Braithwaite and William R. Vollmar

Lewis Research Center
Cleveland, Ohio

NATIONAL AERONAUTICS AND SPACE ADMINISTRATION • WASHINGTON, D. C. • JUNE 1969

PERFORMANCE AND STALL LIMITS OF A YTF30-P-1 TURBOFAN

ENGINE WITH UNIFORM INLET FLOW

By Willis M. Braithwaite and William R. Vollmar

Lewis Research Center
Cleveland, Ohio

NATIONAL AERONAUTICS AND SPACE ADMINISTRATION

ABSTRACT

Performance and operating limits with uniform compressor inlet flow at a Reynolds number index of 0.5 are presented for a YTF30-P-1 (serial number P-647218) two-spool turbofan engine. A description is also included of the high-frequency pressure measurement system developed and the techniques used in this investigation. Results are presented in the form of compressor maps, stall lines, bypass ratio, rotor speed match, and typical time histories.

PERFORMANCE AND STALL LIMITS OF A YTF30-P-1 TURBOFAN ENGINE

WITH UNIFORM INLET FLOW

by Willis M. Braithwaite and William R. Vollmar

Lewis Research Center

SUMMARY

An investigation was conducted to determine the performance and operating limits of the YTF30-P-1 turbofan engine with uniform compressor inlet flow. This engine was selected as being typical of those considered for supersonic aircraft.

Steady-state performance maps are presented for the fan (first three stages) and for the low-pressure compressor (the next six stages). Maps are not presented for the high-pressure compressor (stages 10 to 16) because of damaged 16th-stage rotor blades. The effect of exhaust nozzle area variation and acceleration bleed are shown on the maps.

Stall limits are presented only for the low- and high-pressure compressors; the fan never completely stalled but did encounter rotating stall. The rotating stall was often encountered following compressor stall, and this condition prevented acceleration and normal recovery of the engine.

INTRODUCTION

Operational limits of propulsion systems restrict the flight capabilities of subsonic and supersonic aircraft, and one such limit for gas turbine propulsion systems is compressor stall. The performance and operating limits of the compressor are influenced by the flow conditions at the compressor inlet, which leads to the necessity for compatibility between the induction system and the engine. Thus, a reasonable condition of flow delivered by the inlet and a tolerance of the engine compressor to reasonable inlet flow distortions is essential.

A program to evaluate the influence of steady-state and dynamic compressor inlet disturbances on the operating limits of turbine engines has been initiated at the Lewis Research Center and a YTF30-P-1 two-spool turbofan engine with afterburner was

selected for the first phase. To accomplish the desired evaluation, it was necessary to develop a high-response measurement capability for pressures within and at the inlet and exit of, the compressor. Such capability is required to determine the occurrence of stall and its location within the compressor.

This report presents the performance and operating limits with uniform compressor inlet flow. It includes a description of the high-frequency pressure measurement system used in this investigation. Data were obtained at inlet conditions of half an atmosphere and sea level temperature for a range of rotor speeds and exhaust nozzle areas. The results are presented in the form of compressor maps, stall lines, bypass ratios, rotor speed match, and typical time histories.

APPARATUS

Herein, the engine and the instrumentation design and calibration techniques are described. A brief discussion of the engine installation in the facility is also given.

Engine

The engine was a Pratt and Whitney preproduction YTF30-P-1 (serial number P-647218) twin-spool turbofan equipped with an afterburner. The engine, installed in the altitude test facility, is shown in figure 1. The physical layout of the engine, shown
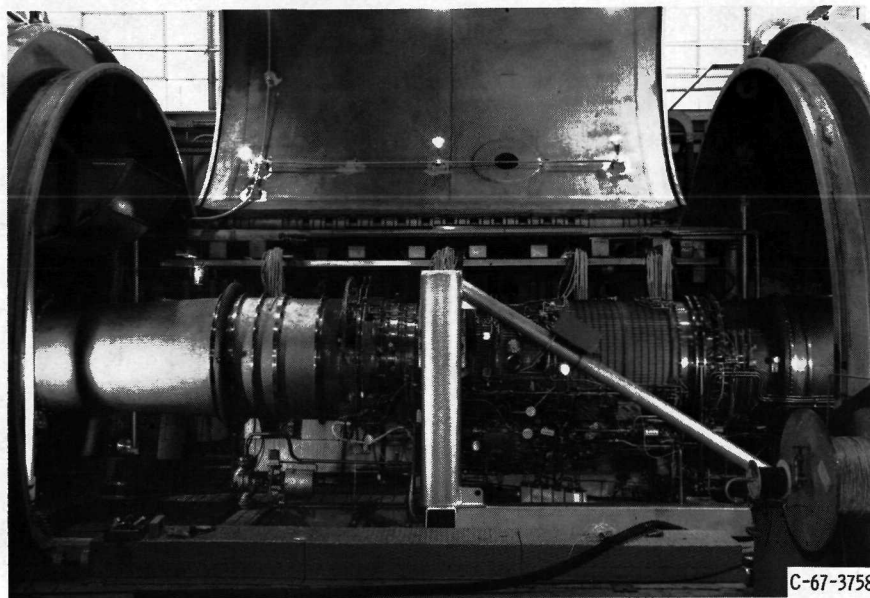

C-67-3758

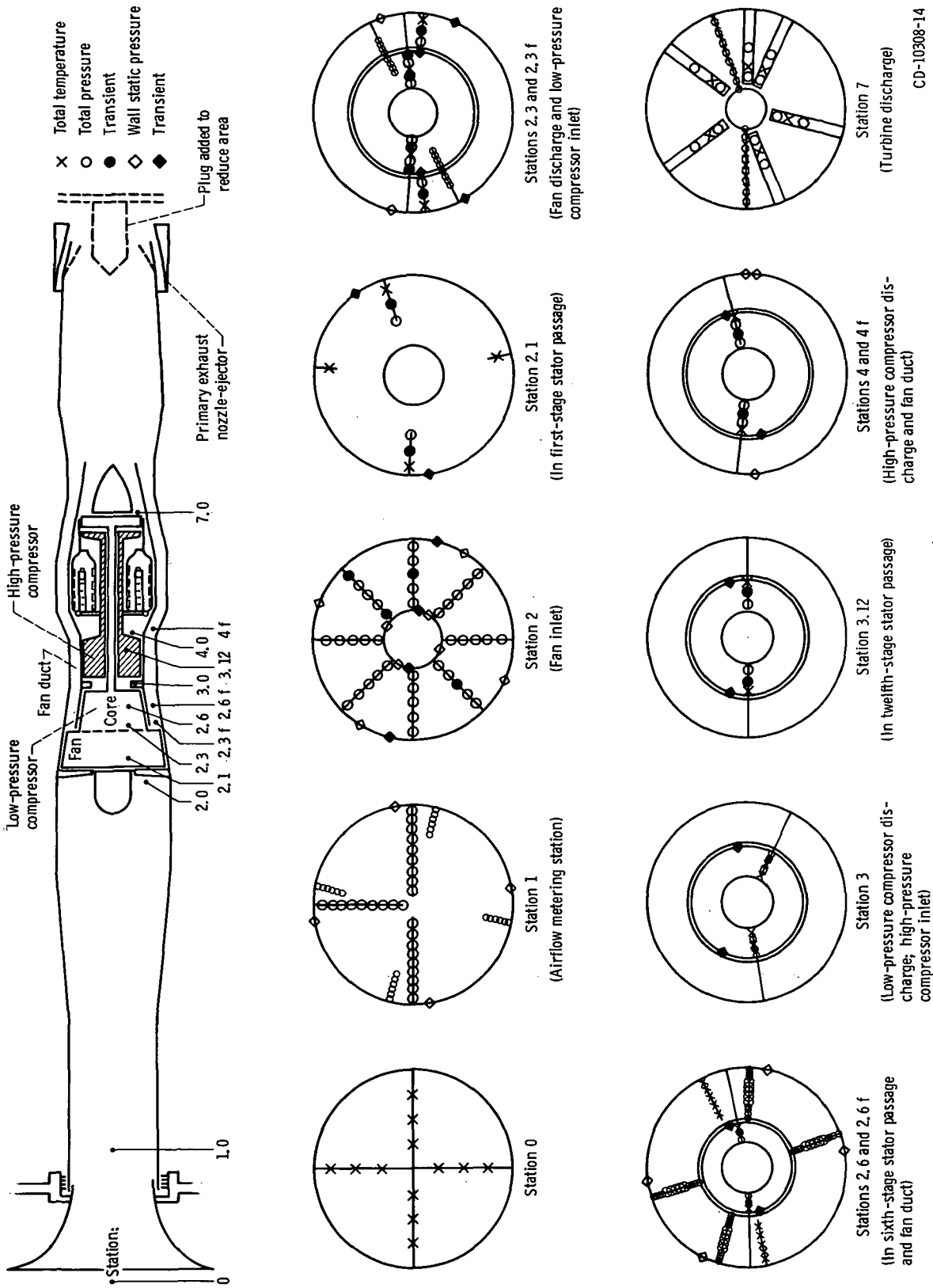Figure 1. - Turbofan engine installed in altitude test chamber.

Total temperature   ×
Total pressure   ○
Transient   ●
Wall static pressure   ◇
Transient   ◆

Plug added to reduce area

Primary exhaust nozzle-ejector

High-pressure compressor

Low-pressure compressor

Fan duct

Core

Fan

Station:

2.0 | 2.3 | 2.3 f | 2.6 | 2.6 f | 3.12 | 4.0
2.1   3.0   3.12   4 f

7.0

1.0

0

Station 0

Station 1
(Airflow metering station)

Station 2
(Fan inlet)

Station 2.1
(In first-stage stator passage)

Stations 2.3 and 2.3 f
(Fan discharge and low-pressure compressor inlet)

Stations 2.6 and 2.6 f
(In sixth-stage stator passage and fan duct)

Station 3
(Low-pressure compressor discharge; high-pressure compressor inlet)

Station 3.12
(In twelfth-stage stator passage)

Stations 4 and 4 f
(High-pressure compressor discharge and fan duct)

Station 7
(Turbine discharge)

CD-10308-14

Figure 2. – Instrumentation layout for YTF30-P-1 turbofan engine.

4876 E-4825

3

schematically in figure 2, consists of a three-stage axial-flow fan mounted on the same shaft with a six-stage, axial-flow, low-pressure compressor. This unit is driven by a three-stage, low-pressure turbine. A seven-stage, axial-flow compressor driven by a single-stage, air-cooled turbine make up the high-speed spool. The nominal overall pressure ratio of the compressor system is 17:1 with a fan bypass ratio of 1. The fan duct airflow is diverted from the core flow by a splitter ring at the exit of the third-stage stators. It then passes through an annular passage surrounding the core engine and is combined with the turbine discharge gases at the afterburner inlet. The total flow is then discharged through a variable-area exhaust nozzle. An ejector nozzle having aerodynamically operated blow-in doors and exit leaves (also called tail feathers) is a part of the normal engine-afterburner configuration. The ejector prevents over-expansion of the primary jet and provides cooling and purging for the engine compartment.

The engine was equipped with automatic 12th-stage bleeds. These bleeds were open at low engine speeds to aid in acceleration and were closed when the pressure differential across the low-pressure compressor reached a predetermined value. This engine also had 5th-stage bleeds (the production models have 6th-stage bleeds).

Engine modifications. - The engine had been modified by the manufacturer to include essentially the same compressor components and fuel control as the production version. It was aerodynamically the same as the production TF30-P-1 engine, except for the bleed location in the low-pressure compressor.

Several modifications were made to the engine to make it more suitable for this investigation. The afterburner fuel system was deactivated and the afterburner control was modified so that the primary exhaust nozzle area could be varied independently from full-closed, or rated (3.78 ft^2, 0.351 m^2), to full open (186 percent of rated). A plug, not supported by the engine, was inserted into the nozzle to obtain effective areas from 72 to 100 percent of the rated area. The blow-in doors were fastened shut and the tail feathers were removed from the ejector.

Another modification was the incorporation of a fuel-step device. An accumulator, which was filled with fuel during normal engine operation, was discharged by pressurizing it with high-pressure gaseous nitrogen. The fuel was injected into the fuel system between the fuel control and the engine. The size of the step could be controlled by the gas pressure used and the length of time that it was supplied to the accumulator.

A modification was also made to the 12th-stage bleed system such that the bleeds could be placed on automatic operation or could be maintained either open or closed as desired. This permitted obtaining data with the bleeds closed at low speeds and open at high speeds.

Engine protection systems. - The danger of damage to the engine resulting from exceeding the turbine inlet temperature or rotor speed limits was minimized by modifying the engine control. When one of these limits was exceeded, a three-way valve inserted

4

in the burner pressure sense line was actuated. This valve vented the control to the test chamber pressure. The control schedules fuel flow as a function of burner pressure. Therefore, the flow was reduced to a minimum value as the pressure at the control was reduced to approximately 1/25 to 1/75 the original value. The automatic restart switch, which senses a rapid change in burner pressure, was also modified such that when stall occurred (a rapid decrease in pressure) the three-way valve was actuated and the fuel flow reduced to the minimum. Each of these detectors also triggered visual and audible alarms when the limits were exceeded.

Instrumentation

The location of the instrumentation used in this investigation is also shown in figure 2. The station identification is shown on this engine schematic and the location and number of measurements at each station are shown on each station sketch. The station locations were selected to divide the compressor into groups of three to four stages each.

Steady state. - Pressures were recorded on a digital automatic multiple pressure recorder having the following pressure ranges:

Station	Range		Accuracy	
	psia	N/cm^2	psi	N/cm^2
1, 2, 2.1, and test chamber	1 to 14	9.6	±0.014	0.0096
2.3, 2.3f, 2.6, 2.6f, 4f, and 7	1 to 35	24	±.035	.024
3, 3.12, 4, and burner	1 to 140	96	±.14	.096

Chromel-Alumel thermocouples were used to measure all temperatures and were recorded on an automatic voltage digitizer. These systems are described in more detail in reference 1.

High-response transient instrumentation. - The location of the high-response pressure transducers is also shown in figure 2. One of the objectives of this program was to have the capability of determining the location of the initiation of stall, to trace its progression through the compressor, and to determine the phase relation between various locations in the compressor. It was estimated that a frequency response of 500 hertz with a maximum of ±5 percent error in amplitude was required. To meet this requirement, the transducer must be located within 1 to 2 inches from the sense point. The presence of the fan duct annulus greatly complicated the instrumentation design and
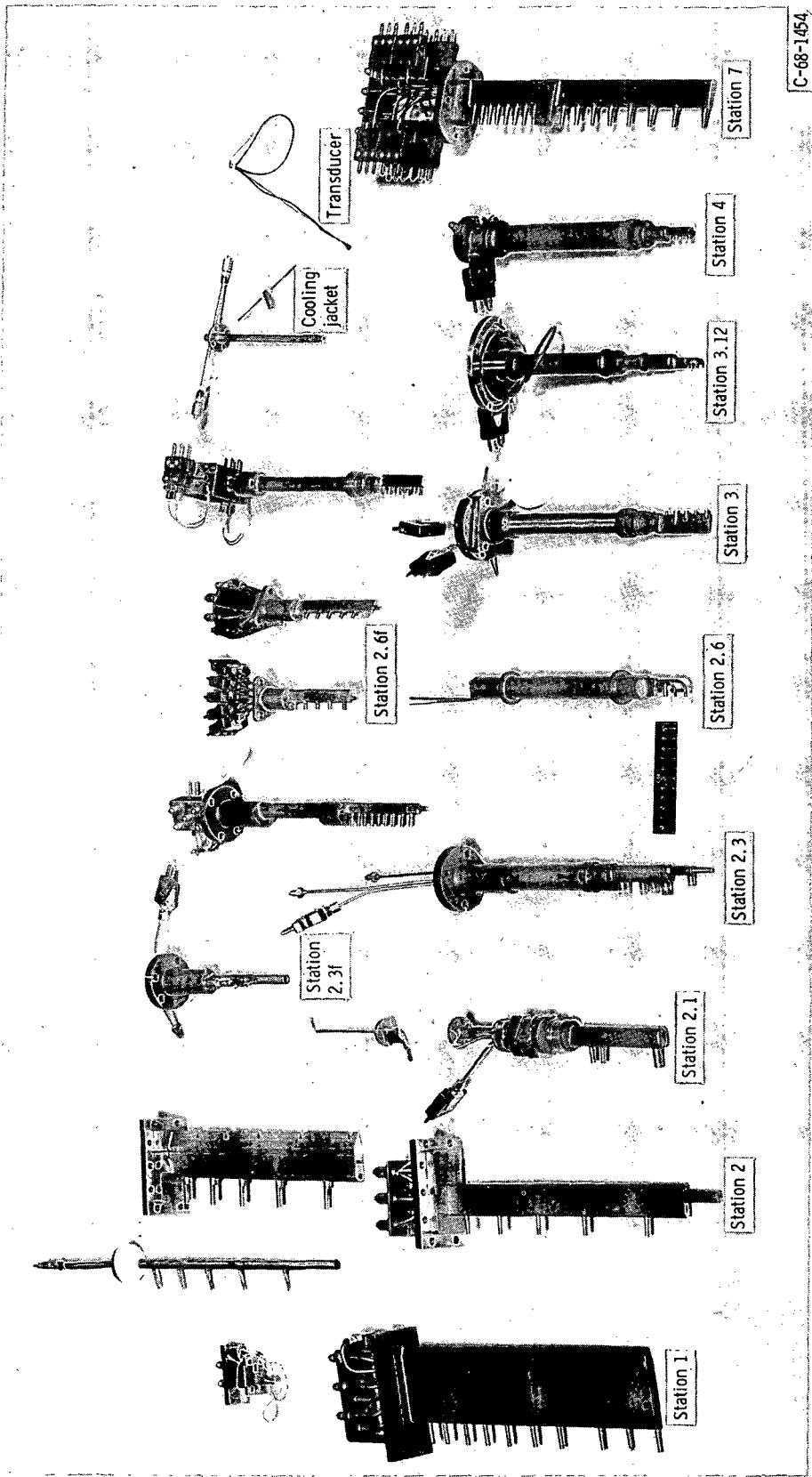
Figure 3. - Rakes containing high-response total-pressure transducers.

C-68-1454

Station 7

Station 4

Station 3.12

Station 3

Station 2.6f

Station 2.6

Station 2.3

Station 2.3f

Station 2.1

Station 2

Station 1

Transducer

Cooling jacket

6

in some cases only a 300- to 350-hertz frequency response was obtainable. Typical probes are shown in figure 3, and a cross section of a typical rake is shown in figure 4. Miniature transducers, 1/4 inch in diameter, were used and were located in the probes at a point that was in, or adjacent to, the gas stream. Because the transducers were limited to a 170° F (76.5° C) operating temperature and had significant calibration shifts with temperature, water cooling was employed. The transducers, mounted in the water jackets, could be removed for repair without removing the complete rake from the engine.

Preliminary calibration of these miniature transducers indicated that zero and sensitivity shifts occurred as a function of time and were not predictable. Thus, it was

CD-10309-14
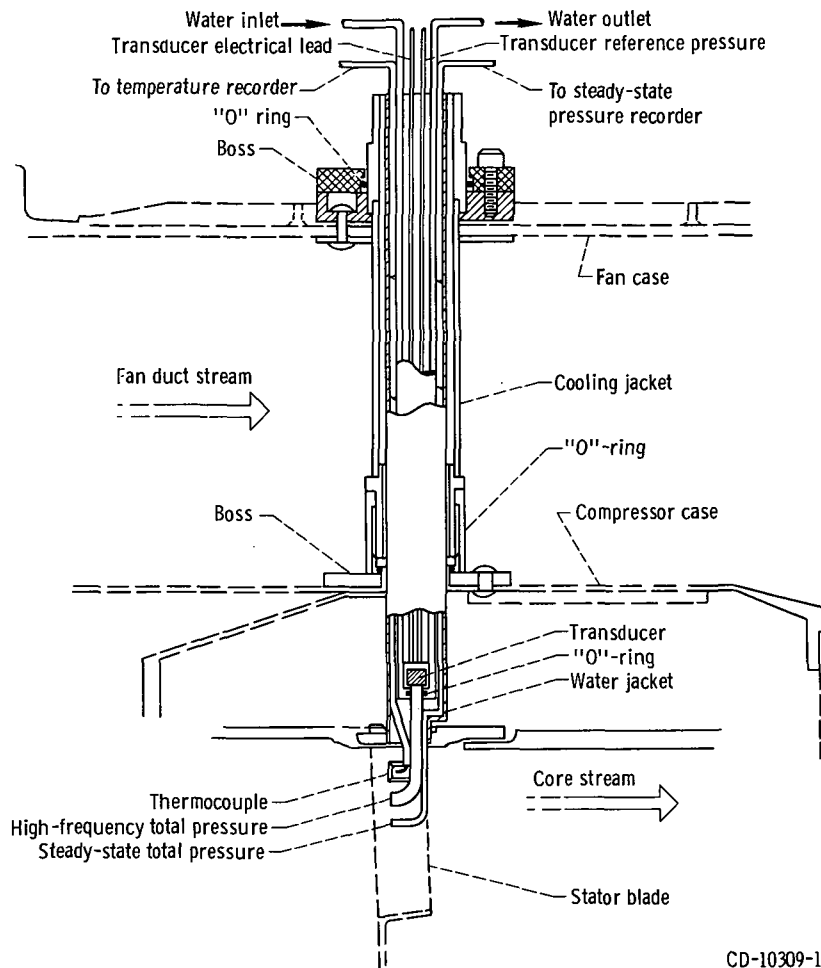
Figure 4. - Typical probe installation.
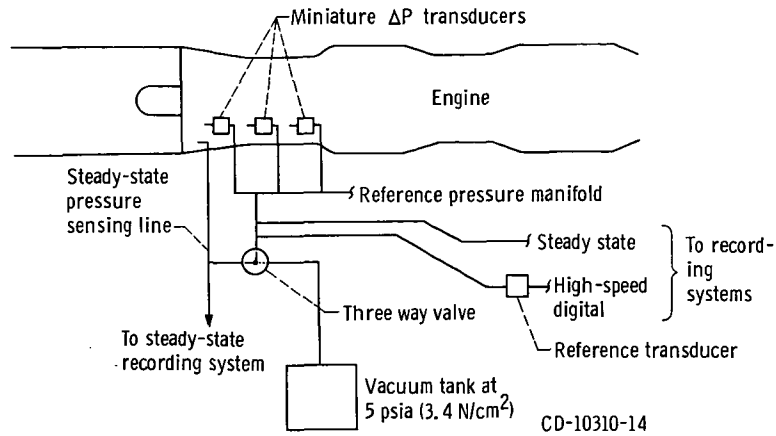
Figure 5. - Reference system used for transient instrumentation calibration.

not possible to trust the prerun calibrations for any extended period of time. Therefore, a system was devised to calibrate these transducers in their operating environment inside the engine just prior to recording transient data. These transducers were only used to measure the pressure change from the steady-state values existing just prior to the transient. A schematic of the calibration system is shown in figure 5.

The calibration of these miniature ΔP transducers consisted of observing the change in output for two values of reference pressure. The engine pressures were held constant by maintaining steady-state conditions. One reference pressure was obtained from the engine by using the normal steady-state pressure probes. The second reference pressure was a constant of approximately 5 psia (3.4 N/cm^2). The sensitivity of the transducers is the ratio of the change in reference pressure to the change in transducer output. The second or 5-psia (3.4-N/cm^2) pressure was maintained during the transient. The base pressure levels for these transient measurements were obtained from an adjacent steady-state, total-pressure measurement or, in the case of the wall static pressures, was computed from the airflow through that station.

The high-frequency response data were recorded simultaneously on a high-speed digitizer-recorder and on magnetic tape. The digital recorder had a sampling rate of approximately 60 samples per second per channel. Therefore, these data were used only to follow the transient up to the point of stall. The actual stall point and time sequence were obtained from the analog traces made from the magnetic tape.

Engine Installation

The engine installation was a conventional direct-connect type (fig. 1). The altitude chamber includes a forward bulkhead which separates the inlet plenum from the test

chamber. Conditioned air was supplied to the plenum at the desired pressure and temperature. The chamber aft of the bulkhead was evacuated to the desired altitude pressure. The conditioned air flowed from the plenum through a bellmouth and duct to the engine inlet. A valve in the bulkhead allowed some air to bypass the engine. The bulkhead valve was automatically controlled to maintain a constant inlet pressure and ram pressure ratio across the engine during steady state and normal engine transient operation. The exhaust from the engine was captured by a collector, extending through a rear bulkhead, to minimize recirculation of the exhaust gases into the test chamber. The exhaust pressure was maintained constant by an automatic valve.

PROCEDURE

Test Conditions

This investigation was conducted at a Reynolds number index of 0.5 (an inlet temperature of 60° F (16° C) and an inlet total pressure of 7.5 psia (5.2 N/cm^2)). Ram pressure ratio across the engine was held constant at 3:1 to assure a choked exhaust nozzle for all operating conditions. These test conditions were selected for several reasons. First, this Reynolds number index corresponds to a range of flight Mach numbers and altitudes representative of the flight regime of supersonic aircraft. A second reason is that the loss in performance due to Reynolds number effect would not be expected to be significant (as determined from the engine manufacturer's test data). Also, the pressure loadings on the instrumented case would be reduced, and this pressure level would simplify the data acquisition problem.

Steady-State Data

The steady-state data required for mapping the compressors' performance were obtained by operating the engine at a number of points throughout the speed range from idle to military speed, limiting low rotor speed, or limiting turbine inlet temperature, for each of six exhaust nozzle areas. These areas ranged from 72 to 186 percent of rated area of 3.78 square feet (0.351 m^2). These points were obtained for operation with the 12th-stage bleeds in both the closed and open positions. The 5th-stage bleeds, which are not standard for production models of the engine, were closed for all the data presented herein. The basic data obtained are presented in the figures in the appendix.

Stall Data

Two techniques were used to induce stall in the compressor units. The low-pressure compressor operating line was raised toward the stall limit by increasing the exhaust nozzle area above rated. The engine was then very slowly accelerated (10 to 20 rpm/sec) until the engine either stalled as indicated by a rapid change in rotor speed and turbine inlet temperature or reached one of the operating limits. In a similar manner, the exhaust nozzle was closed to raise the operating lines of the high-pressure compressor and fan. Again, a slow acceleration was made until stall occurred or an operational limit was reached. The slow acceleration was used to keep the engine close to the steady-state operating line for the particular nozzle size. Data were recorded from the transient instrumentation during these slow accelerations from the last stable operating point prior to stall.

The second method of inducing stall was to inject an increment of fuel into the engine fuel system. The resulting fuel step would cause a step increase in pressure at the high-pressure compressor exit. The size of the fuel step was increased until stall was obtained. Fuel steps induced stall in the high compressor and were made from three or four selected steady-state speed points between idle and maximum.

Data Processing

Steady-state performance was computed for each compressor stage group for which there were data and for each compressor component in terms of pressure ratios across the unit, efficiencies, corrected airflows, and corrected rotor speeds. Total airflow was computed by the area-weighted summation of airflow per unit area obtained from individual total-pressure measurements at station 1 assuming that the measured average total temperature and wall static pressure existed in a one-dimensional fashion across the duct. There were six total-pressure measurements in the boundary layer next to the wall. The fan duct airflow was calculated in a similar manner at station 2.6f. In this case, five boundary layer probes were used adjacent to each of the inner and outer walls. The core flow was defined as the difference between the total and fan duct flows. The bypass ratio was defined as the ratio of the fan duct airflow to the core airflow.

The transient data recorded on the digital system were plotted as time histories of pressures, temperatures, pressure ratios, efficiencies, and corrected rotor speeds. The temperatures recorded during fuel step transients were compensated for the thermocouple time lag resulting from the rapid temperature change. No compensation was necessary for the slow acceleration data.

The data recorded on the magnetic tape were played back in analog form at time expansion of 16:1. This provided the required time resolution for determination of the in-

ception of stall and its progression through the compressors. The peak values of pressure and corresponding speeds were obtained from these traces.

RESULTS AND DISCUSSION

Steady-State Performance

The boundary assumed between the core and fan duct flow in the fan is somewhat arbitrary due to the lack of a physical flow separator until after the flow has left the third stage. The fan includes the first three stages, and the low-pressure compressor the next six. However, the performance of the outer annulus of the fan is a different function of the exhaust nozzle area than is that of the inner annulus. Therefore, the fan performance is presented by means of two sets of maps. The performance of the outer fan annulus is presented as the pressure ratio $P_{t,2.6f}/P_{t,2}$ (fan duct total pressure to inlet total pressure) as a function of corrected total airflow $W_{a,t}\sqrt{\theta_2}/\delta_2$ and corrected fan speed $N_1/\sqrt{\theta_2}$ (fig. 6). The inner annulus performance is defined by the pressure ratio $P_{t,2.3}/P_{t,2}$ (fourth stage inlet to engine inlet total pressure) as a function of corrected total airflow and corrected fan speed (fig. 7). The bypass ratio, the ratio of fan duct airflow to core airflow, is presented in figure 8.

Performance of the low-pressure compressor, stages 4 to 9, is presented in figure 9 as the total-pressure ratio $P_{t,3}/P_{t,2.3}$ (ninth stage exit to fourth stage inlet) as a function of corrected core airflow $W_{a,t}\sqrt{\theta_{2.3}}/\delta_{2.3}$ and corrected low rotor speed, $N_1/\sqrt{\theta_{2.3}}$.

High-compressor data are presented in the form of total-pressure ratio $P_{t,4}/P_{t,3}$ as a function of corrected high rotor speed $N_2/\sqrt{\theta_3}$ in the discussion of stall. These data are not necessarily typical of the YTF30-P-1 engine inasmuch as disassembly of the engine subsequent to this investigation disclosed that the 16th-stage rotor shroud was dented inward at one circumferential location and the tips of the rotor blades were worn away about 0.07 inch (fig. 10). Because of the increased clearance, the performance and operating limits of the high-pressure compressor are not considered representative of the normal compressor. The resulting match between the high and low rotor speeds is presented in figure 11 as $N_2/\sqrt{\theta_3}$ as a function of $N_1/\sqrt{\theta_2}$ and $N_2/\sqrt{\theta_2}$, the controlled speed.

Fan performance. - Fan performance is presented in the form of maps in figure 6 for the outer annulus and in figure 7 for the inner annulus. Separate maps are presented for the 12th-stage bleeds closed and open.
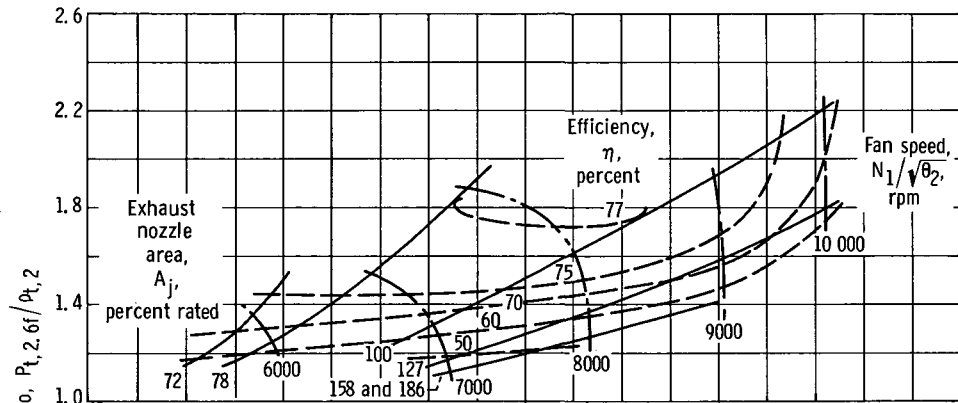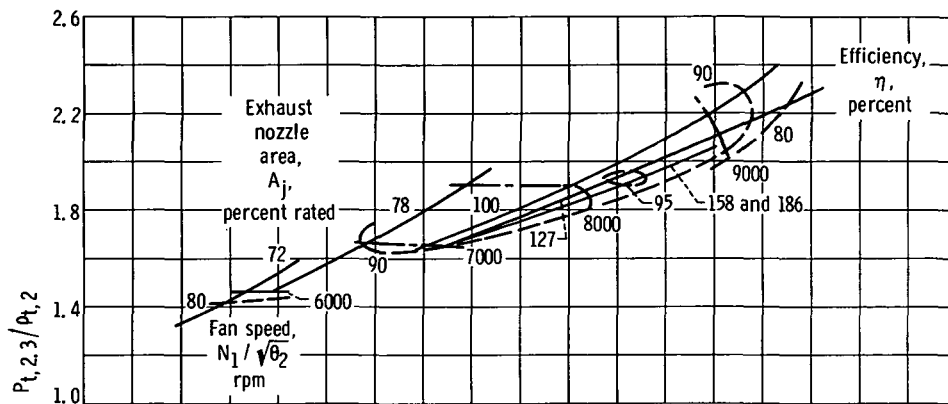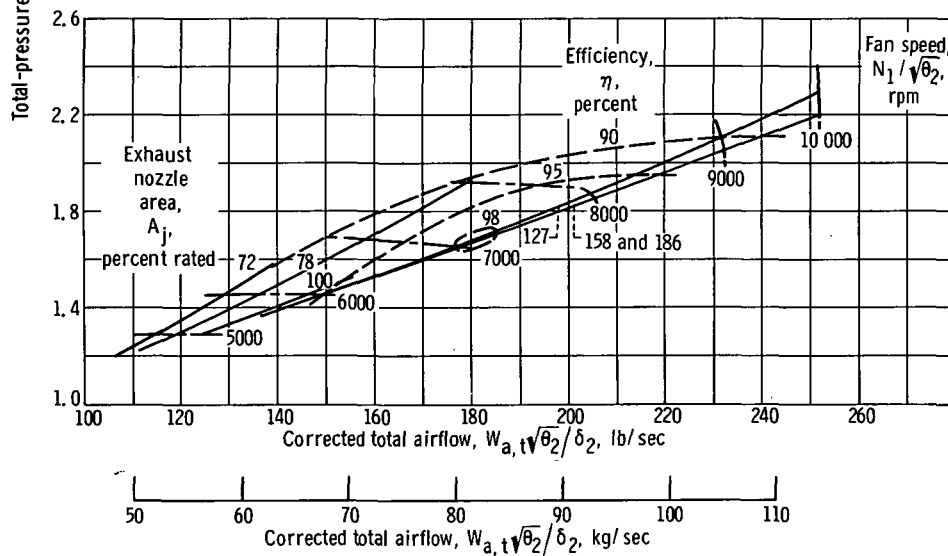
(a) Twelfth-stage bleeds closed.
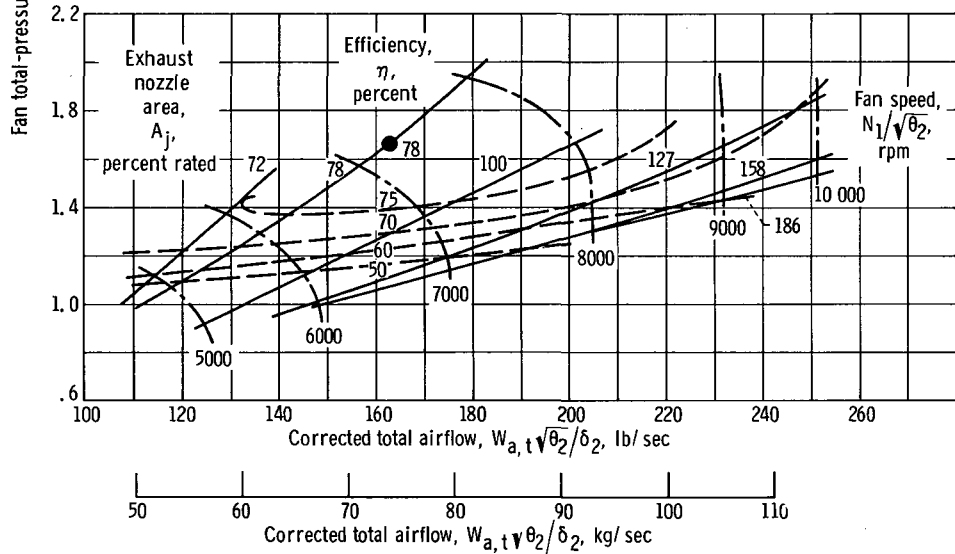
(b) Twelfth-stage bleeds open.

Figure 6. – Fan map for outer annulus of YTF30-P-1 turbofan engine at Reynolds number index of 0.5.

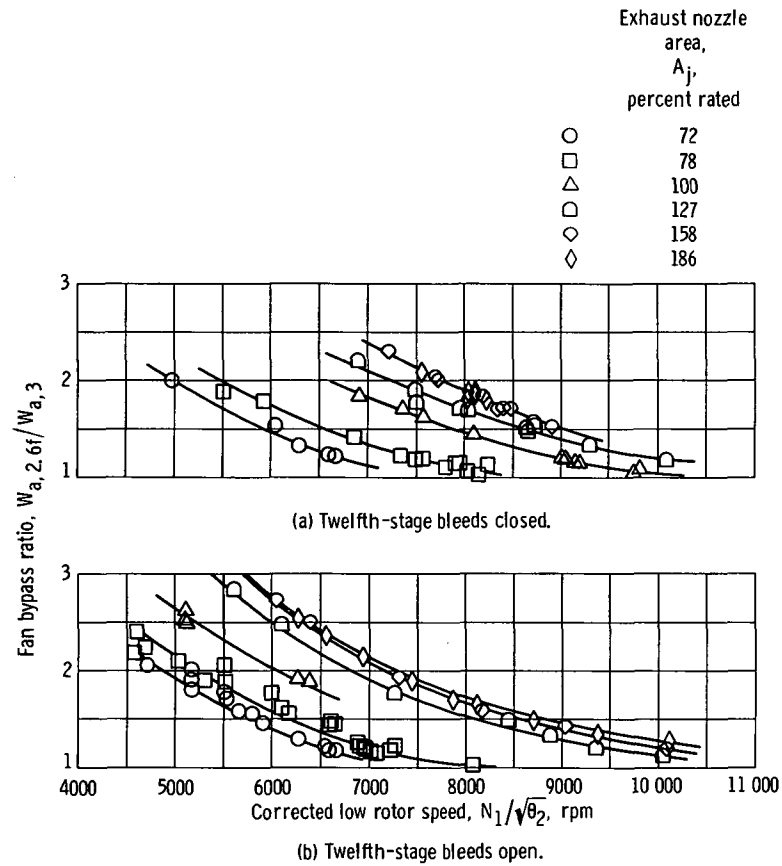Figure 7. - Fan map for inner annulus of YTF30-P-1 turbofan engine at Reynolds number index of 0. 5.
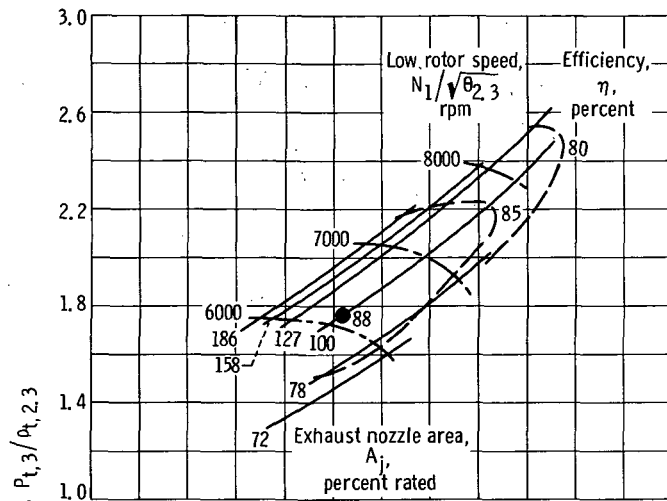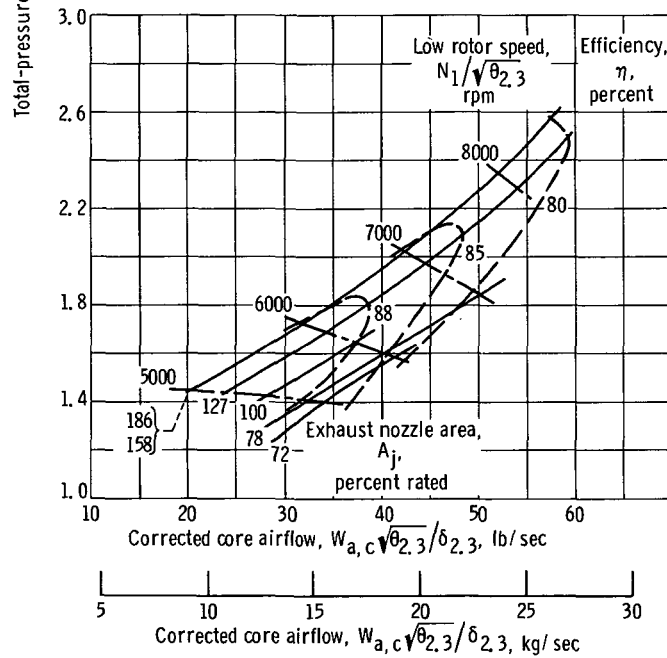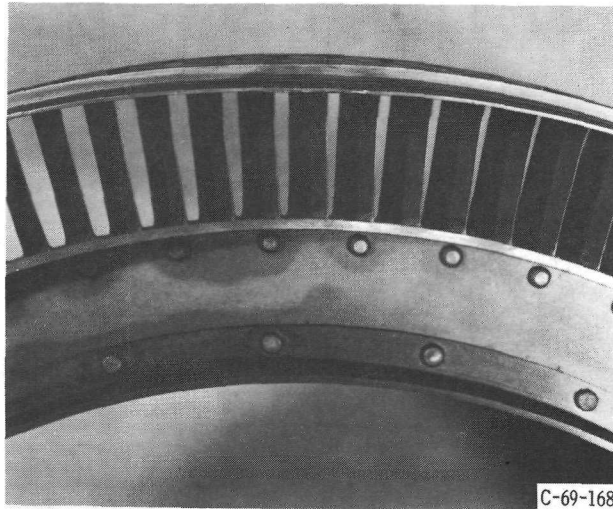
Figure 8. – Fan bypass airflow characteristics for YTF30-P-1 turbofan engine at Reynolds number index of 0. 5.
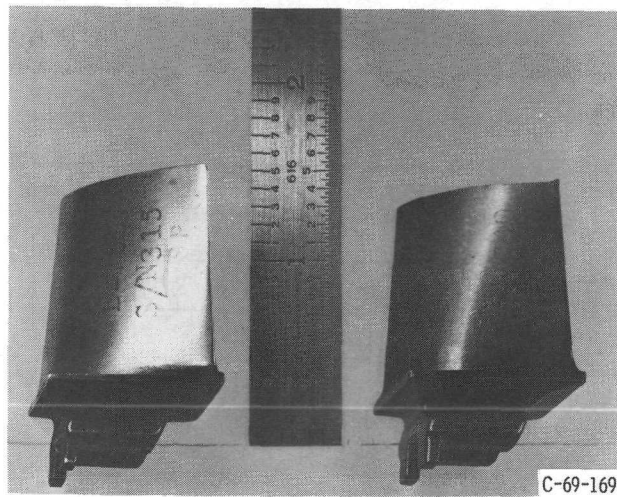
(a) Twelfth-stage bleeds closed.

(b) Twelfth-stage bleeds open.

Figure 9. – Low-pressure compressor map for YTF30-P-1 turbofan engine at Reynolds number index of 0.5. Stages 4 to 9.

(a) Fifteenth-stage stator showing local outer shroud deformation.

(b) Sixteenth-stage compressor blade with excessive tip wear shown next to new blade.

Figure 10. - Excessive wear and deformation of YTF 30-P-1 turbofan engine.
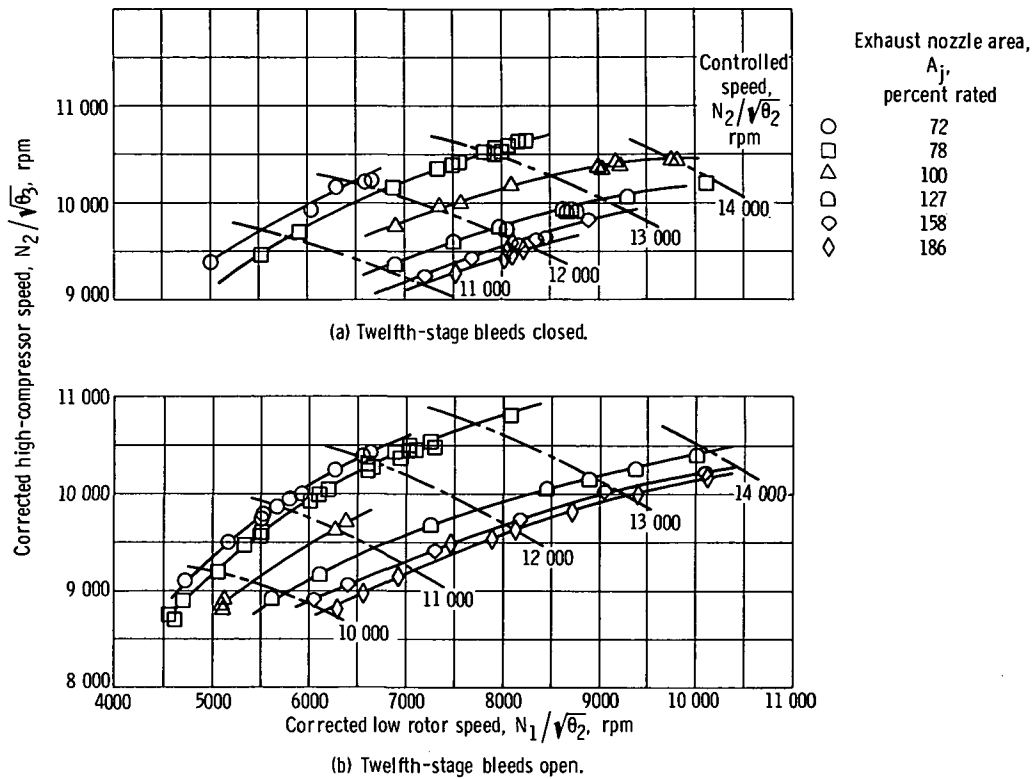
Figure 11. - Rotor speed match for YTF30-P-1 turbofan engine at Reynolds number index of 0.5.

For both the inner and outer parts of the fan, increasing the exhaust nozzle area at a given corrected fan speed resulted in an increase in the corrected inlet total fan flow and a decrease in total-pressure ratio. In general, opening the 12th-stage bleeds resulted in only small changes in the pressure ratio and total airflow for a given speed. The peak isentropic efficiency was lower for the fan outer annulus (about 78 percent compared to approximately 95 percent for the inner annulus) and occurred at lower corrected speeds when the 12th-stage bleeds were opened. These results are based on rather limited instrumentation which was incapable of evaluating the radial profile at the fan exit.

Comparison of the outer and inner fan maps (figs. 6 and 7) indicate that the total-pressure ratio decrease with increasing exhaust nozzle area was greater for the outer annulus than for the inner annulus. The constant corrected speed lines of the inner annulus indicated a constant total-pressure ratio for exhaust nozzle areas below rated and only a slight decrease above rated.

Bypass ratio (fig. 8) increased as exhaust nozzle area was increased at a given corrected low rotor speed and as corrected low rotor speed was reduced at a given exhaust nozzle area. As bypass ratio increased, the fraction of total airflow increased through

17

the fan duct and decreased through the core section. The individual flows are presented in the appendix.

Low-pressure compressor performance. - Maps are presented in figure 9 of the total-pressure ratio $P_{t,3}/P_{t,2.3}$ as a function of core flow and speed corrected to the 4th-stage inlet with the 12th-stage bleeds in both the closed and open positions.

The constant exhaust nozzle operating lines shifted in the direction of reduced pressure ratio for a given corrected flow as the exhaust nozzle area was reduced or the 12th-stage bleeds were opened. The effect of the bleeds was more pronounced with the larger exhaust nozzles. This trend, contrary to that observed in the outer fan annulus, is the result of the matching between the turbines and compressors. Opening the exhaust nozzle increased the pressure drop across the low-pressure turbine. This resulted in more work being done in the low-pressure compressor (i. e., a greater pressure rise and reduced core flow). The effect on the fan was to decrease the pressure ratio and to increase the fan duct airflow.

Normally, the inlet to the low-pressure turbine was choked. Therefore, variations in exhaust nozzle area would have only an indirect effect, due to the change in low-compressor airflow and pressure rise, on the high rotor speed. The match between the two rotor speeds (fig. 11) shows that the low rotor speed increases for a given corrected high rotor speed when the exhaust nozzle area was increased. Opening the 12th-stage bleeds only slightly influenced the effect of the exhaust nozzle area.

Compressor Stall

Analysis of the transient data to obtain stall pressure ratios and corrected speeds was made in two steps: (1) to identify the stage group that stalled first; and (2) to determine the pressure ratio and corrected speed for this unit immediately prior to stall. Identification of the unit stalling first was made from the analog total pressure time histories. A drop in the discharge and a corresponding rise in the inlet pressure of the group of stages or unit identified it as stalling first. Pressure drops downstream and sequential pressure rises upstream of the unit also aided in locating this unit.

The pressure ratio and corrected speed of the stalling unit were taken from the computed output of the high-speed digital system when stalls were obtained with slow accelerations. For the fuel step transient data, the rate of pressure change was too great; therefore, these pressure ratios were determined from the analog time histories.

A method of analysis has been used in reference 2 for determining the stall pressure ratio of stages ahead of the stage that stalls initially. The flow in the stalled stage is reduced or stagnated. If this occurs rapidly enough, the pressure at the exit of the preceding stage will rise before the inlet pressure and flow of that stage is affected. Thus, this stage, in turn, stalls; and the process is repeated until the stall reaches the inlet of

18

the engine. The fuel step technique initiates stalls in the downstream stages of the high-pressure compressor. Therefore, with this method, the stall pressure ratio of each stage group would be determined from one transient.

Fan stall data (outer annulus) were not obtained since the high-pressure compressor stalled first when the exhaust nozzle area was reduced. The indicated stall margin of the high-pressure compressor was less than normal for this model compressor; this was probably due to the damaged 16th stage.

Typical time histories of pressures in the compressors are shown in figure 12 for three types of stalls observed: (1) a slow acceleration to low-pressure compressor stall with the large exhaust nozzle area, 186 percent; (2) a slow acceleration with a small exhaust nozzle area, 78 percent, to high-pressure compressor stall; and (3) fuel step resulting in high-pressure compressor stall with an exhaust nozzle area of 78 percent. Figure 12(a), a slow acceleration to low-pressure compressor stall, shows a rise in $P_{t, 2.6}$ and a dropoff in $P_{t, 3}$ occurring shortly before the abrupt changes in the other pressures indicating the initiation of stall in that stage group. The decrease in $P_{t, 3.12}$ was not accompanied by a corresponding rise in $P_{t, 3}$; therefore, stall was not considered to have occurred between stations 3 and 3.12. The progression of stall forward from station 2.6 to 2.3, 2.1, and finally 2 is also shown. Figure 12(b), a slow acceleration to high-compressor stall, shows a simultaneous rise in $P_{t, 3.12}$ and a drop in $P_{t, 4}$, indicating that the stall originated between those locations. For this case, the pressure changes forward from the stalling unit occur in less time than for low-pressure compressor stall. The fuel step induced stall, shown in figure 12(c), shows a slight peak in $P_{t, 3.12}$ just prior to stall which is prior to the peak in $P_{t, 3}$ indicating that the last stage or last group of stages stalled first. The peak-to-peak time interval from station 4 to 2 is approximately 0.005 second and is of the same order as that from station 3.12 to 2 shown in figure 12(b).

Low-pressure compressor. - Stall data for the low-pressure compressor are presented in figure 13. The stall data shown for large exhaust nozzle areas were obtained with slow acceleration and with the 12th-stage bleeds closed. With the bleeds open there was sufficient stall margin (as a result of a lower operating line) to prevent stalling the low-pressure compressor with this technique. Lower speed stall data were obtained by tracing the stall forward from the high-pressure compressor. These data were obtained with the 12th-stage bleeds both open and closed. The bleeds did not appear to have any significant effect on the stall line. The two methods of inducing stall yielded data which are in good agreement. The steady-state performance data presented in figure 13 are for the 12th-stage bleeds closed.

The constant-area operating lines for 158 and 186 percent of rated exhaust nozzle area intersected the stall line at corrected speeds between 7500 and 8500 rpm. The stall line had a knee at approximately 8000 rpm.
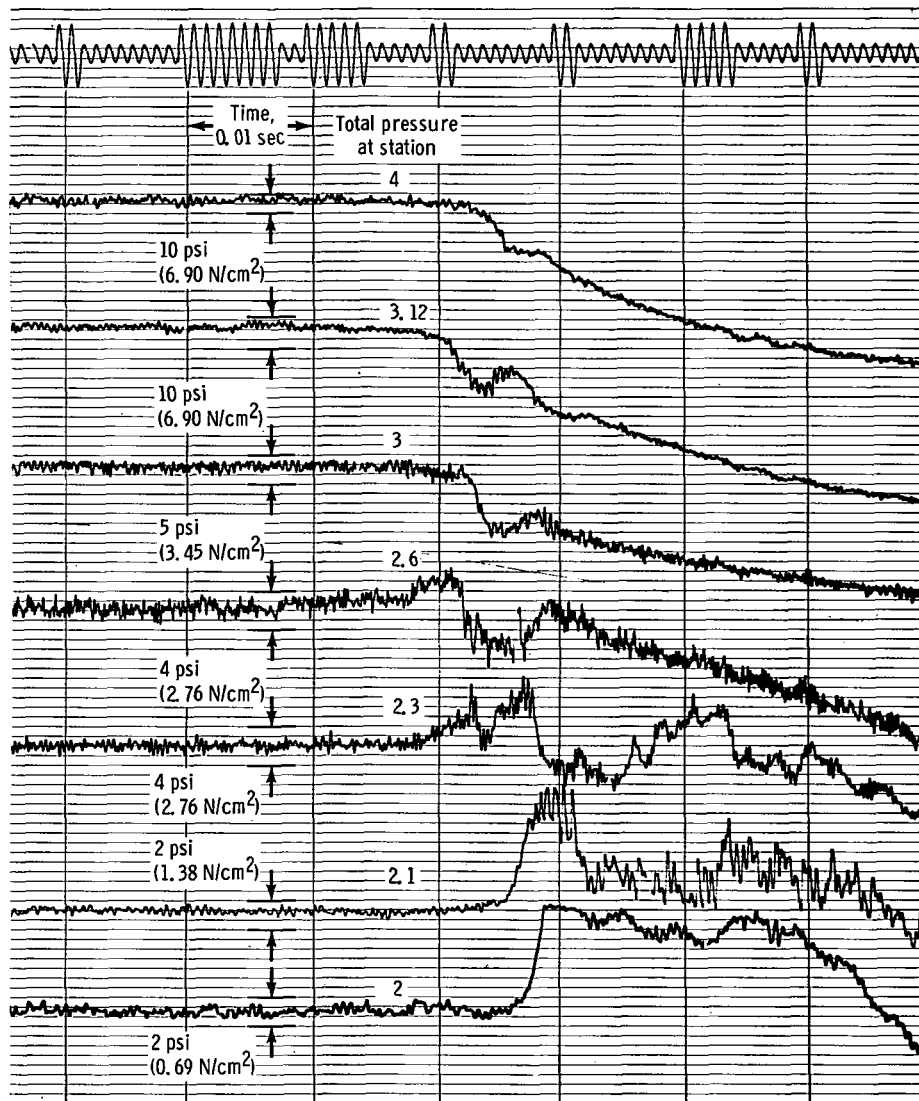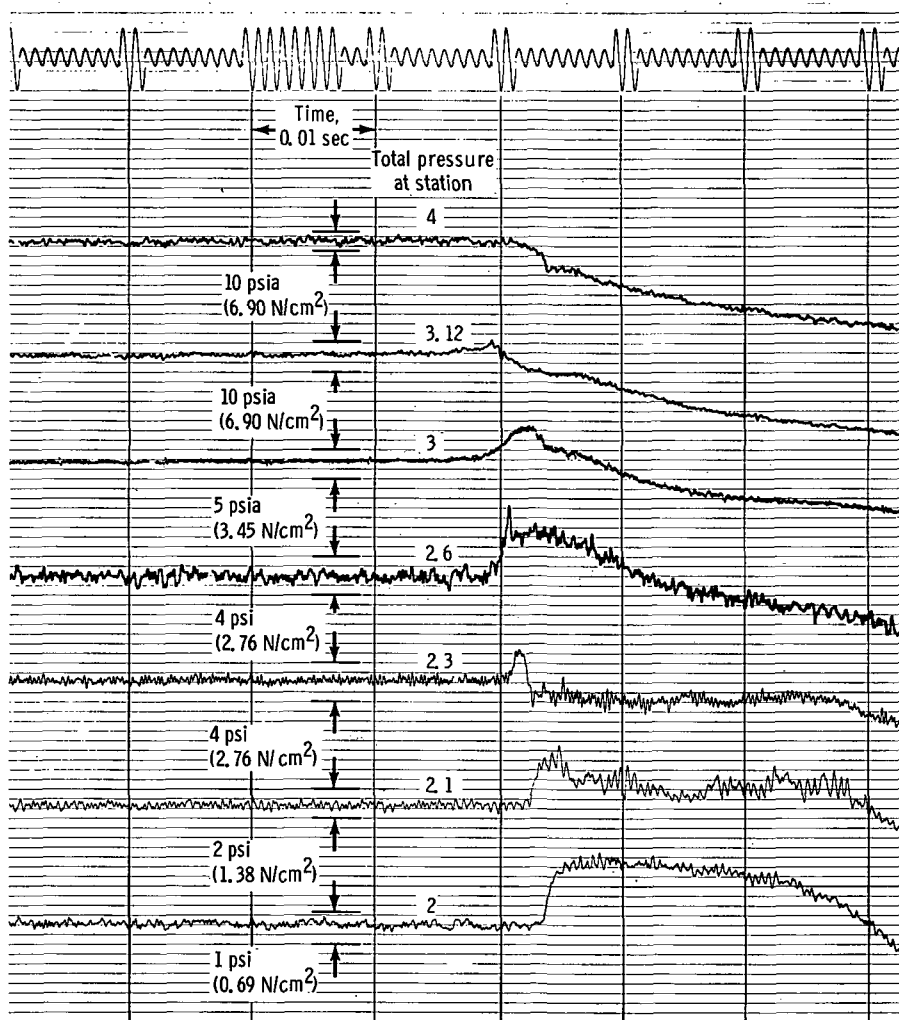
(a) Low-pressure compressor stall. Low rotor speed, 73 percent; exhaust nozzle area, 186 percent rated.

Figure 12. - Typical time histories during stall transient of YTF30-P-1 turbofan engine at Reynolds number index of 0. 5.
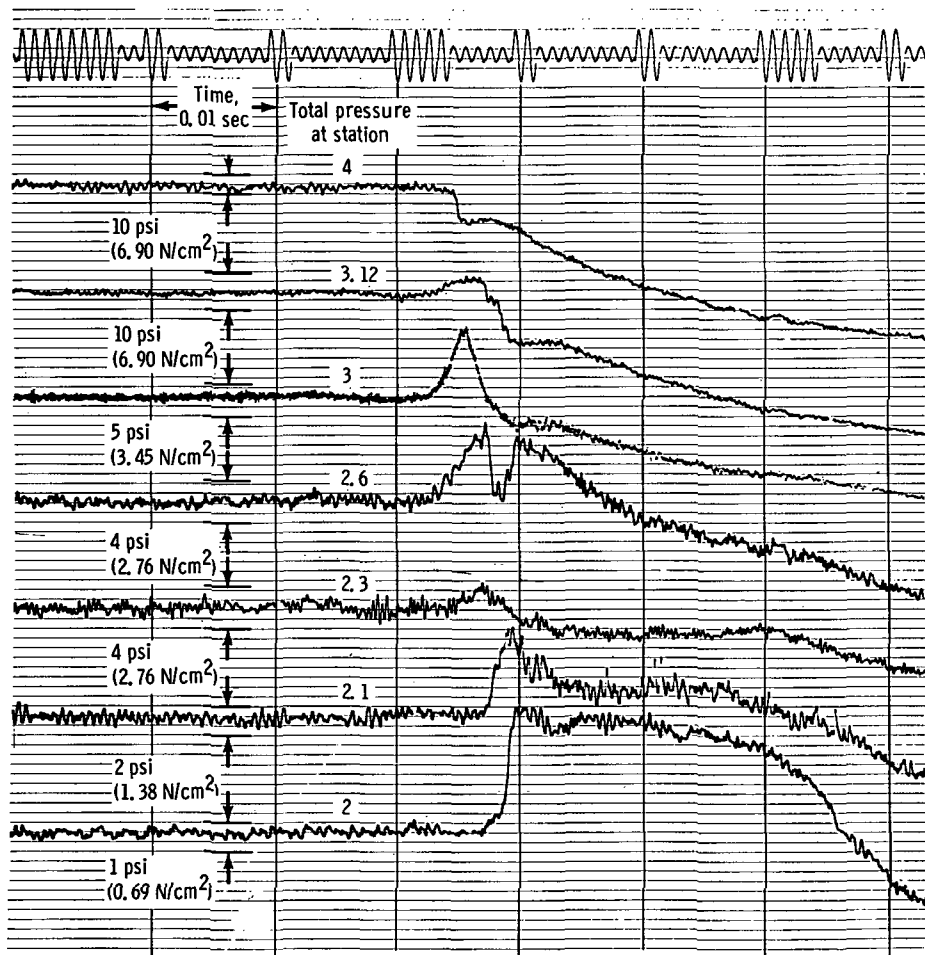
(b) High-pressure compressor stall. High rotor speed, 97 percent; exhaust nozzle area, 78 percent rated.

Figure 12. - Continued.

(c) Fuel-step-induced stall. High rotor speed, 97 percent; exhaust nozzle area, 78 percent rated.
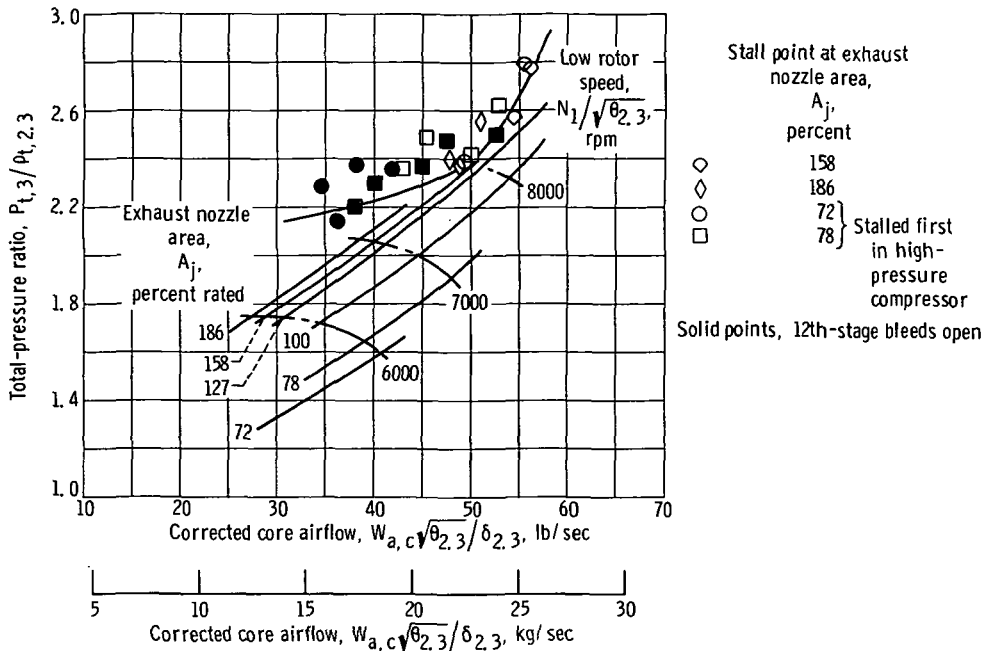
Figure 12. - Concluded.

Figure 13. - Stall characteristics of low-pressure compressor of YTF30-P-1 turbofan engine at Reynolds number index of 0.5.

Two methods may be used to define stall margin. Stalls resulting from back pressure disturbances can be evaluated in terms of pressure ratios as defined by the equation:

$$\text{Stall margin I} = 100 \left(\frac{PR_s}{PR_0} - 1 \right)$$

where PR_s is the stall line pressure ratio at a given corrected speed and PR_0 is the pressure ratio at that speed on the normal operating line. This stall margin for the low-pressure compressor is 3 percent at a corrected rotor speed of 8000 rpm (fig. 13). The second definition takes into account the mass flow margin in addition to the pressure ratio and is defined as

$$\text{Stall margin II} = 100 \left(\frac{W_0}{W_s} \times \frac{PR_s}{PR_0} - 1 \right)$$

where W_0 is the flow rate of the operating line and W_s is the flow rate at stall. The other terms are as defined previously, all at the same constant corrected rotor speed. This stall margin for the low-pressure compressor is 11 percent at 8000 rpm.
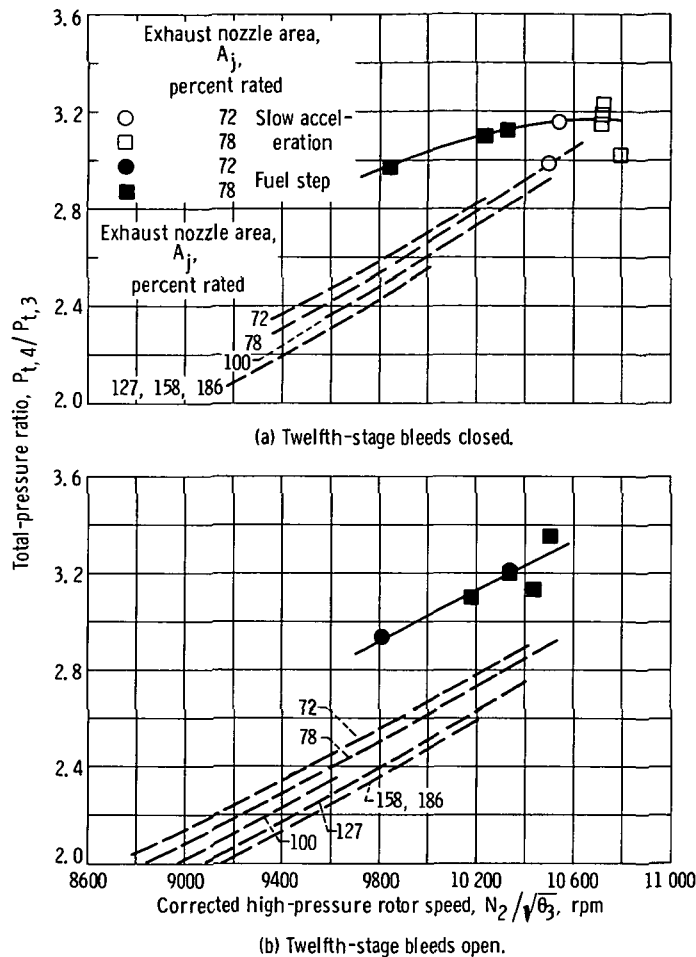
Figure 14. – High-pressure compressor stall characteristics of YTF30-P-1 turbofan engine at Reynolds number index of 0. 5.

High-pressure compressor. - The high-pressure compressor data are presented as a plot of total-pressure ratio against corrected high rotor speed in figures 14(a) and (b) for the 12th-stage bleeds closed and open, respectively. Stall data obtained with both slow accelerations and fuel steps are shown. As mentioned previously, these data are not considered valid or representative of the normal compressor of this type. However, some observations may be made. There was only a very small increase in stall pressure ratio at the high corrected rotor speeds when the 12th-stage bleeds were opened. The steady-state operating line, however, was lowered which resulted in increasing the pressure-ratio stall margin of this compressor for operation with rated exhaust nozzle area from 13 to 16 percent at a constant corrected speed of 10 200 rpm.

The two methods of inducing stall gave comparable results. The fuel step method permitted obtaining stall data at lower speeds and with the 12th-stage bleeds open.
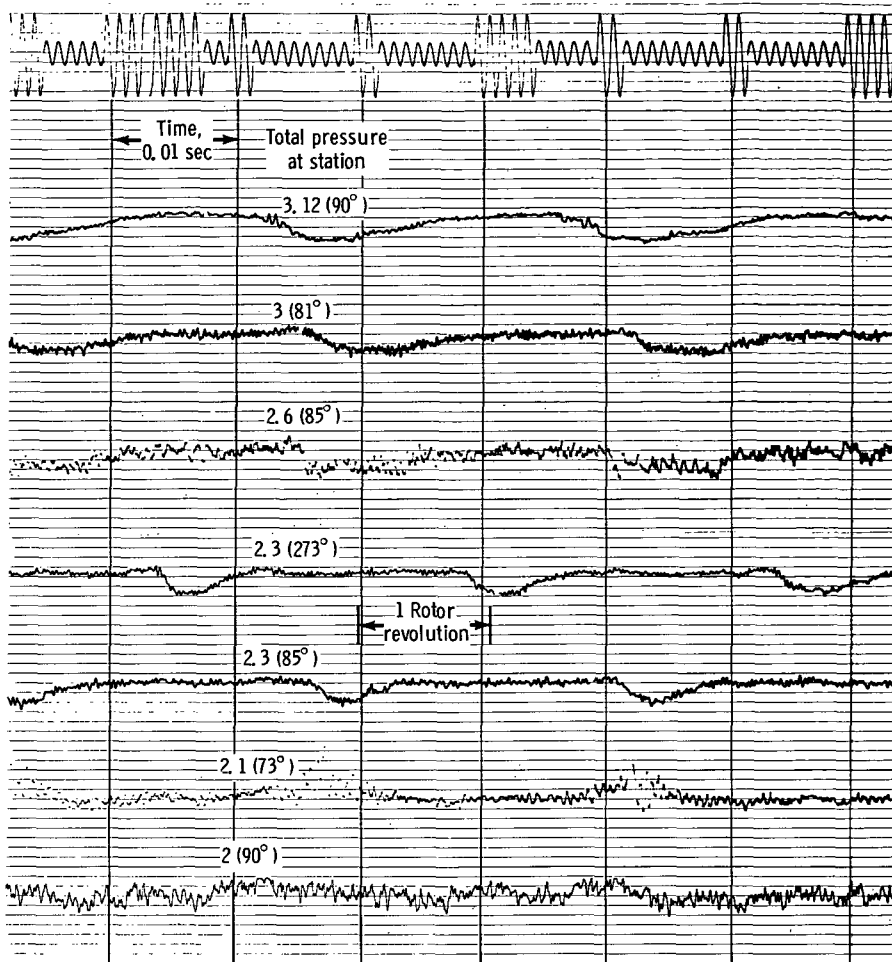
Figure 15. - Typical rotating stall pattern observed in YTF30-P-1 turbofan engine following compressor stall. Low rotor speed, 56 percent, high rotor speed, 77 percent; exhaust nozzle area, 186 percent rated. Reynolds number index, 0.5; stall frequency, 0.43 low rotor frequency.

Rotating stall. - A deep rotating stall condition often existed following the compressor stalls. When this happened the compressor pressures fluctuated (fig. 15), the low rotor speed decreased, and the turbine inlet temperature increased from the normal value determined by the power setting. A single-zone pattern was indicated to be rotating at 43 percent of low rotor speed. The 180° phase shift indicated by the two $P_{t,2.3}$ traces, approximately 180° apart, confirmed the one-zone pattern. At stations 2 and 2.1, a pressure rise occurred when the stall zone passed while all the pressures downstream dropped, indicating that the rotating stall occurred after the first fan stage and that the stall zone, or its influence, was present in the following stages of both the low- and high-pressure compressors.

The engine could not be accelerated above a high rotor speed of 11 800 rpm while in rotating stall. This was due to the acceleration schedule limit of the fuel control. The
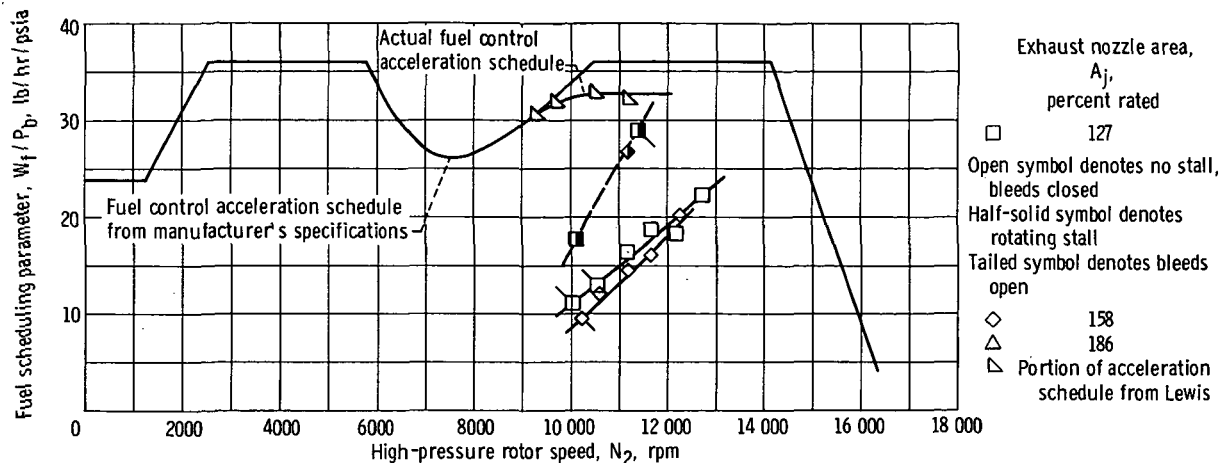
Figure 16. - Fuel schedule for YTF30-P-1 turbofan engine. Total temperature at station 2, 59° F (15° C).

fuel schedule parameter, ratio of fuel flow rate to burner pressure, for steady-state operation in rotating stall is approximately double the normal requirement (fig. 16). Also shown in this figure are experimentally determined acceleration limit points for the fuel control used for this investigation. The steady state with rotating stall line intersected this limit line at about 11 800 rpm, preventing any further acceleration.

Operationally it was difficult to clear the rotating stall from the engine. Either the engine had to be shut down or a variety of manipulations of ram ratio (reduction), altitude, 12th-stage bleeds, and exhaust nozzle area made to clear the stall. The most successful method was to shut down the engine and restart after a few seconds of windmilling.

CONCLUDING REMARKS

An investigation was conducted to determine the performance and operating limits of a YTF30-P-1 turbofan engine with uniform compressor inlet flow. This engine was selected as being typical of those for use in supersonic aircraft.

The last stage of the high-pressure compressor was found to be damaged upon disassembly. Therefore, the performance and operating limits of this unit are not necessarily representative of the normal compressor of this type.

The results may be summarized as follows:

1. The fan total-pressure ratio decreased or remained constant and the corrected total airflow increased as the exhaust nozzle area increased at a given corrected fan speed; the total-pressure ratio decreased more rapidly in the outer annulus than it did in the inner or core section. The bypass ratio increased for increasing exhaust nozzle area as a result of the fan duct airflow increasing while the core flow decreased.

26

2. The low-pressure compressor total-pressure ratio increased and the corrected core airflow decreased with increasing exhaust nozzle area at a given corrected low rotor speed. There was a small decrease in total-pressure ratio when the 12th-stage bleeds were opened. Compressor stall was encountered at exhaust nozzle areas of 158 and 186 percent of rated at corrected speeds between 7500 and 8500 rpm. The stall margin was 3 percent based on pressure ratio or 11 percent based on both pressure ratio and mass flow at a corrected low rotor speed of 8000, the knee in the stall line.

3. It was possible to stall the high-pressure compressor of this particular engine by reducing the exhaust nozzle area, as well as by means of fuel steps. Opening the 12th-stage bleeds increased the pressure-ratio stall margin from 13 to 16 percent at 10 200 rpm, primarily by lowering the steady-state operating line.

4. Following complete compressor stall, a single-zone rotating stall was frequently present and prevented acceleration of the engine above 11 800 rpm high rotor speed. The stall or its effects were present in all core and fan stages.

5. The experimental techniques and high-response instrumentation developed for this program were found to be highly effective in determining the type of stall, its origin, and its progression through the compressor system.

Lewis Research Center,
    National Aeronautics and Space Administration,
        Cleveland, Ohio, January 8, 1969,
            720-03-00-09-22.

APPENDIX - BASIC PERFORMANCE DATA

The basic performance data obtained for the YTF30-P-1 turbofan engine, serial number P-647218, are presented as corrected airflow, total-pressure ratios, and compressor efficiencies as functions of corrected rotor speed and exhaust nozzle area in figures 17 to 24. Separate curves are included for the 12th-stage bleeds open.
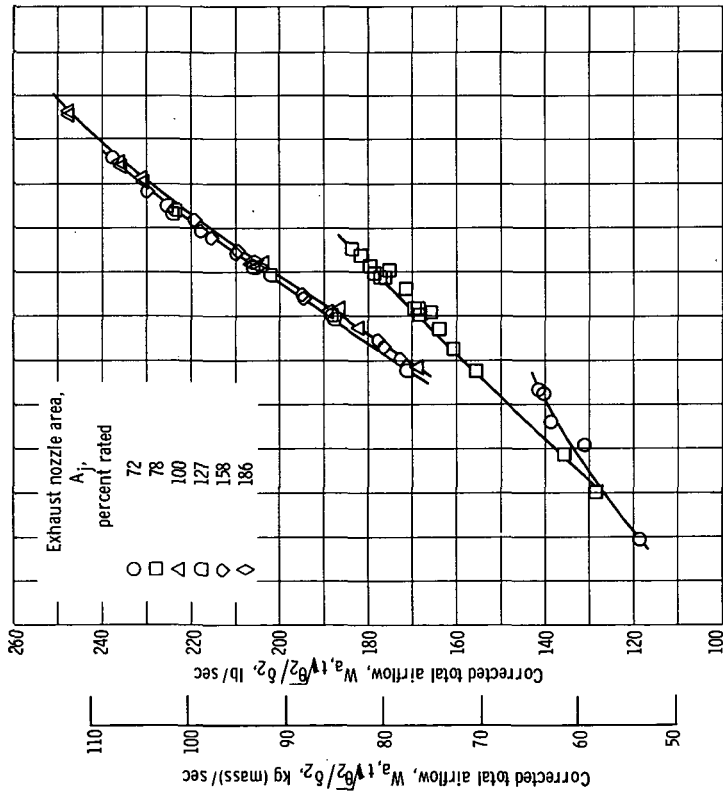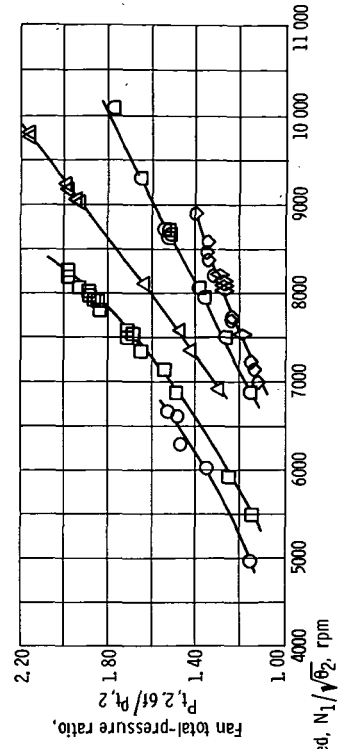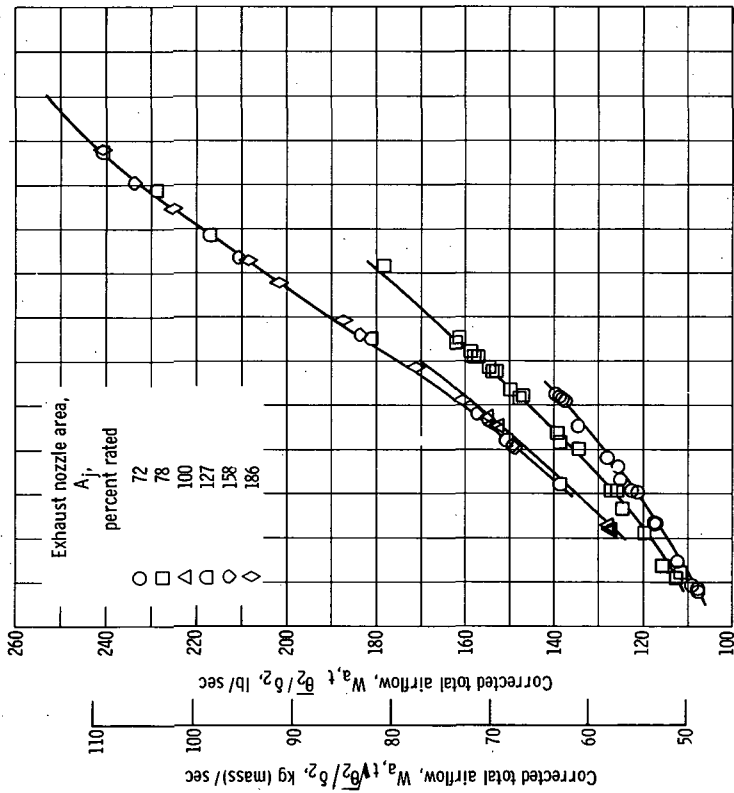
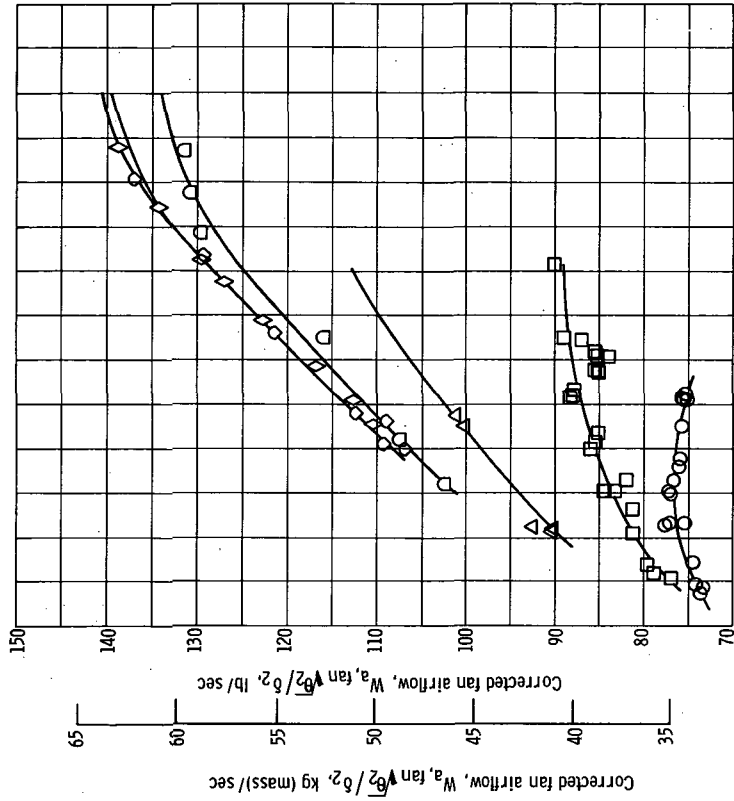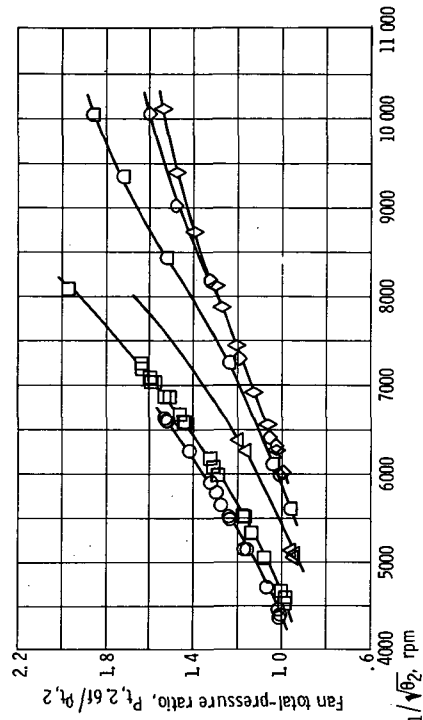(a) Total airflow.
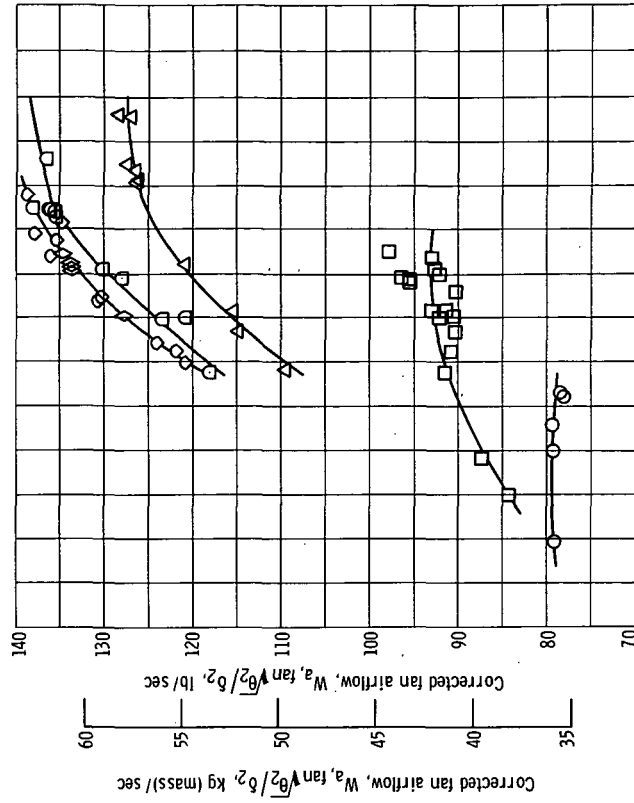
(b) Fan airflow.
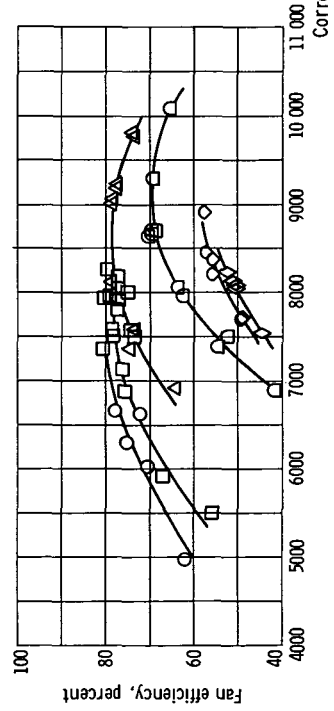
(c) Efficiency

(d) Total-pressure ratio.

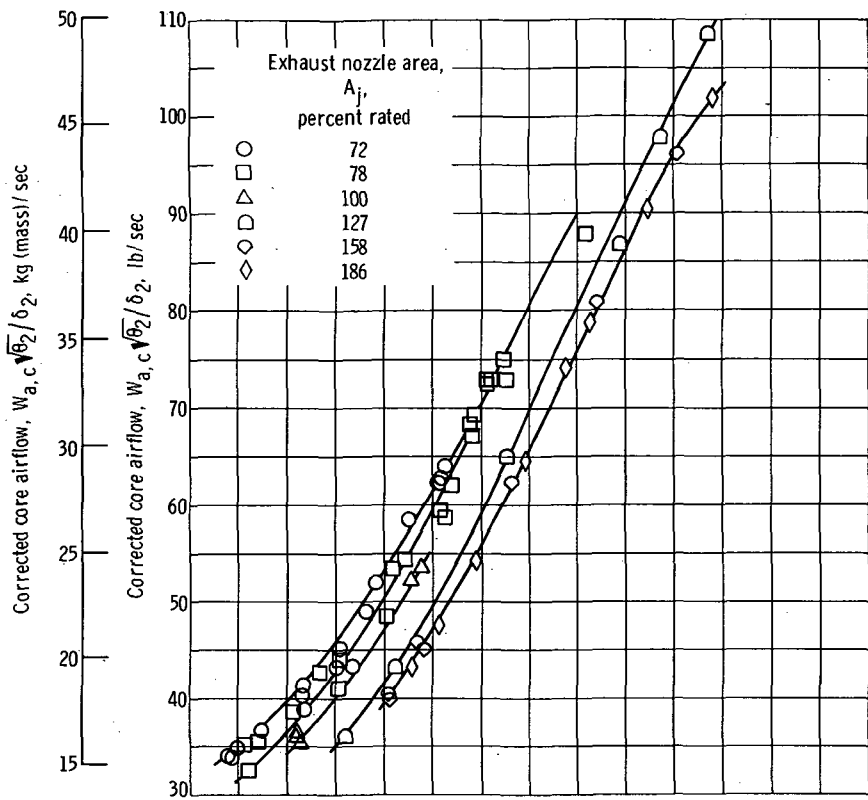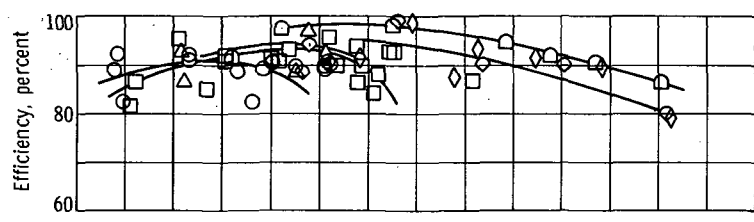Figure 17. – Performance of fan of YTF30-P-1 turbofan engine at Reynolds number index of 0.5, 12th-stage bleed closed.

Exhaust nozzle area,
A_j,
percent rated

○	72
□	78
◁	100
◖	127
◇	158
◇	186

Corrected total airflow, $W_{a,t}\sqrt{\theta_2}/\delta_2$, lb/sec

Corrected total airflow, $W_{a,t}\sqrt{\theta_2}/\delta_2$, kg (mass)/sec

Corrected fan airflow, $W_{a,fan}\sqrt{\theta_2}/\delta_2$, lb/sec

Corrected fan airflow, $W_{a,fan}\sqrt{\theta_2}/\delta_2$, kg (mass)/sec

Fan efficiency, percent

Fan total-pressure ratio, $P_{t,2.6f}/P_{t,2}$

Corrected fan speed, $N_1/\sqrt{\theta_2}$, rpm

29

(a) Total airflow.

(b) Fan airflow
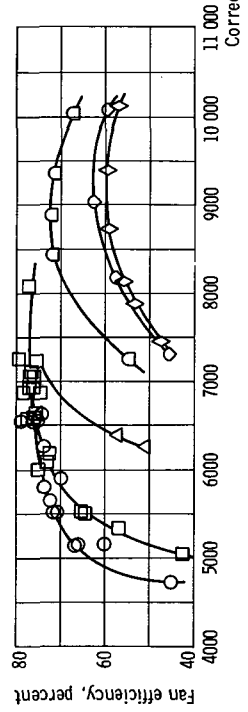
(c) Efficiency.

(d) Total-pressure ratio.

Figure 18. – Performance of fan of YTF30-P-1 turbofan engine at Reynolds number index of 0.5, 12th-stage bleed open.
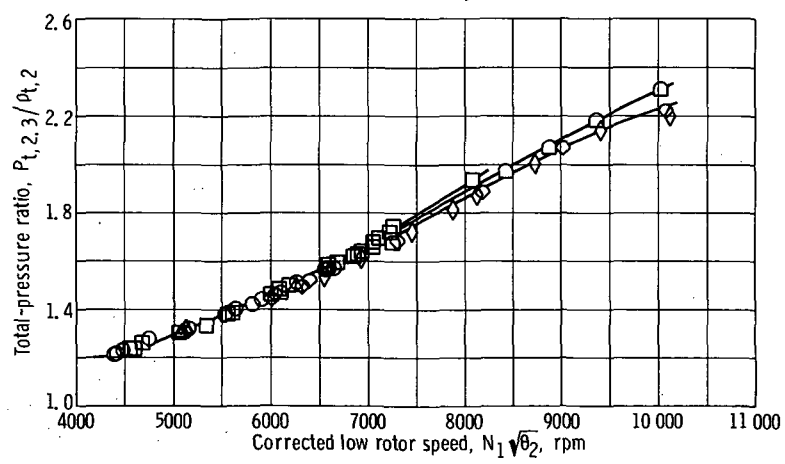
30
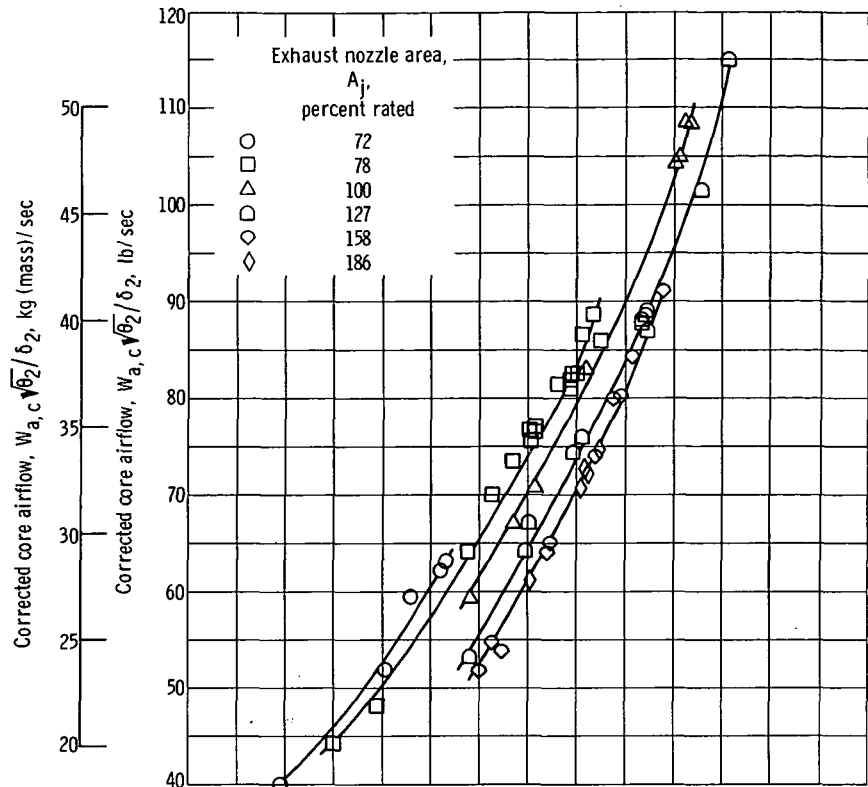
Figure 19. - Performance of core stages 1 to 3 of YTF30-P-1 turbofan engine at Reynolds number index of 0.5, 12th-stage bleed closed.
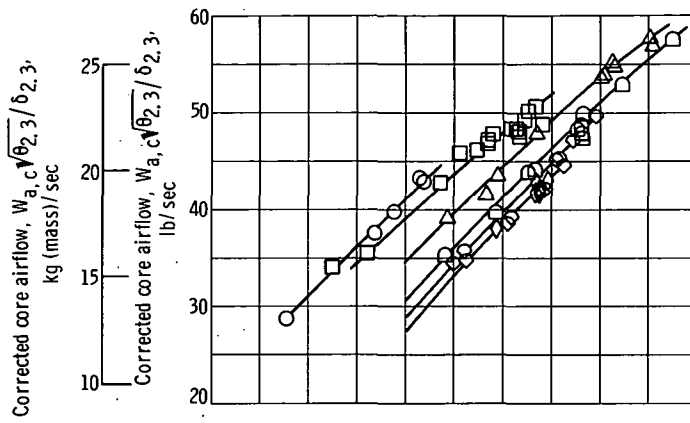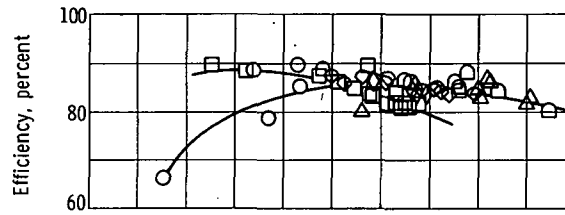
31

(a) Core airflow.
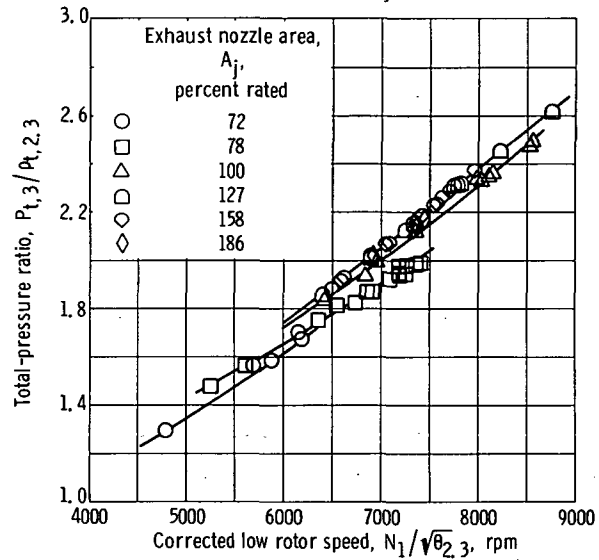
(b) Efficiency.

(c) Total-pressure ratio.

Figure 20. - Performance of core stages 1 to 3 of YTF30-P-1 turbofan engine at Reynolds number index of 0.5, 12th-stage bleed open.
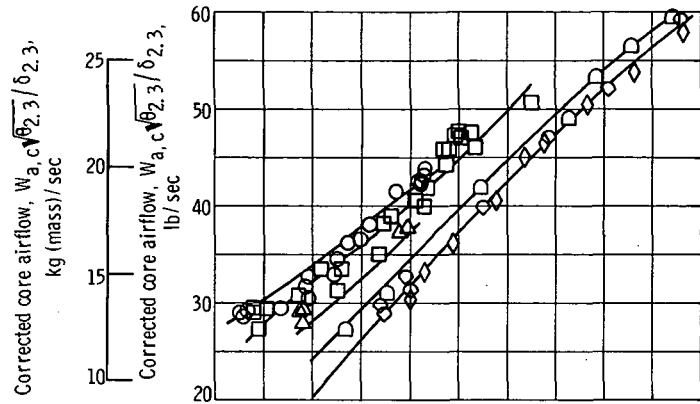
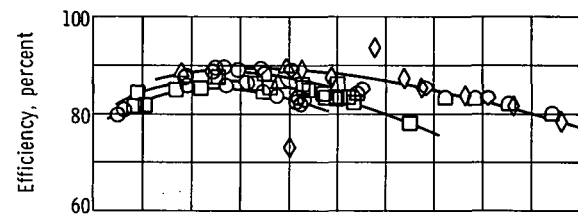(a) Core airflow.

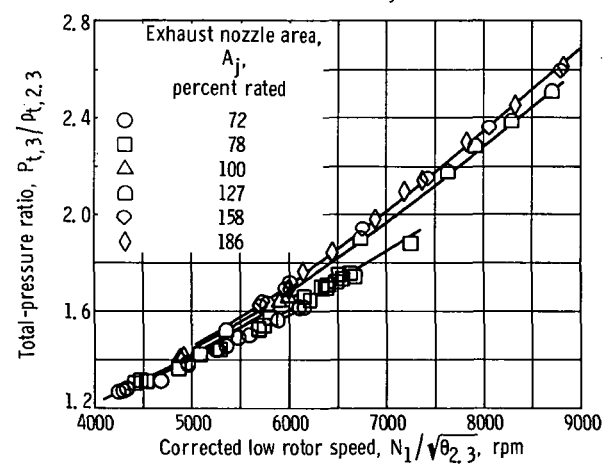(b) Efficiency.

(c) Total-pressure ratio.

Figure 21. - Performance of core stages 4 to 9 of YTF30-P-1 turbofan engine at Reynolds number index of 0.5, 12th-stage bleed closed.

(a) Core airflow.

(b) Efficiency.

Exhaust nozzle area,
A_j,
percent rated

○	72
□	78
△	100
◠	127
◇	158
◊	186

(c) Total-pressure ratio.

Figure 22. - Performance of core stages 4 to 9 of YTF30-P-1 turbofan engine at Reynolds number index of 0.5, 12th-stage bleed open.
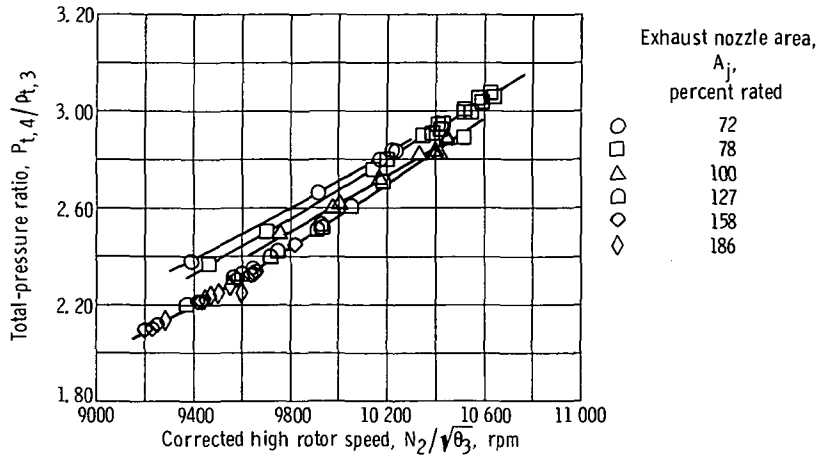
Figure 23. – Performance of high-pressure compressor of YTF30-P-1 turbofan engine at Reynolds number index of 0.5, 12th-stage bleed closed.
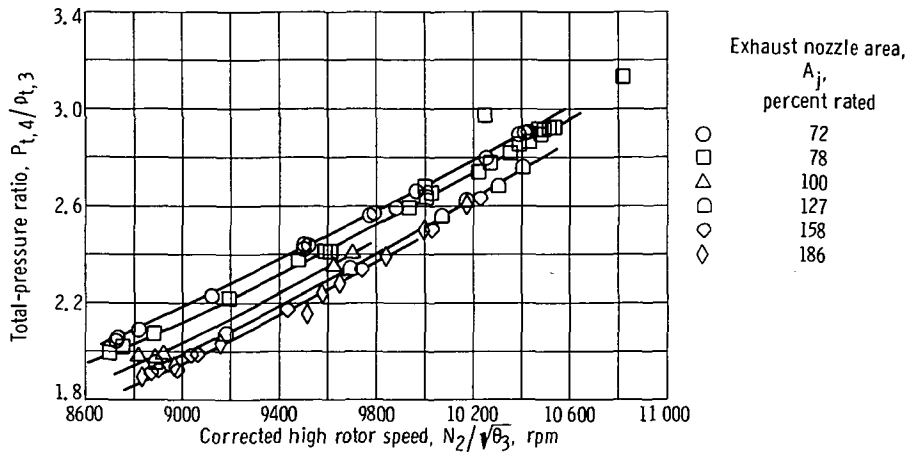

Figure 24. – Performance of high-pressure compressor of YTF30-P-1 turbofan engine at Reynolds number index of 0.5, 12th-stage bleed open.

REFERENCES

1. Staff of Lewis Laboratory: Central Automatic Data Processing System. NACA TN 4212, 1958.

2. Lubick, Robert J.; and Wallner, Lewis E.: Stall Prediction in Gas-Turbine Engines. J. Basic Eng., vol. 81, no. 3, Sept. 1959, pp. 401-408.

"The aeronautical and space activities of the United States shall be conducted so as to contribute . . . to the expansion of human knowledge of phenomena in the atmosphere and space. The Administration shall provide for the widest practicable and appropriate dissemination of information concerning its activities and the results thereof."

— NATIONAL AERONAUTICS AND SPACE ACT OF 1958

NASA SCIENTIFIC AND TECHNICAL PUBLICATIONS

TECHNICAL REPORTS: Scientific and technical information considered important, complete, and a lasting contribution to existing knowledge.

TECHNICAL NOTES: Information less broad in scope but nevertheless of importance as a contribution to existing knowledge.

TECHNICAL MEMORANDUMS: Information receiving limited distribution because of preliminary data, security classification, or other reasons.

CONTRACTOR REPORTS: Scientific and technical information generated under a NASA contract or grant and considered an important contribution to existing knowledge.

TECHNICAL TRANSLATIONS: Information published in a foreign language considered to merit NASA distribution in English.

SPECIAL PUBLICATIONS: Information derived from or of value to NASA activities. Publications include conference proceedings, monographs, data compilations, handbooks, sourcebooks, and special bibliographies.

TECHNOLOGY UTILIZATION PUBLICATIONS: Information on technology used by NASA that may be of particular interest in commercial and other non-aerospace applications. Publications include Tech Briefs, Technology Utilization Reports and Notes, and Technology Surveys.

Details on the availability of these publications may be obtained from:

SCIENTIFIC AND TECHNICAL INFORMATION DIVISION

NATIONAL AERONAUTICS AND SPACE ADMINISTRATION
Washington, D.C. 20546